

5G green cellular networks considering power allocation schemes

Xiaohu GE¹, Jiaqi CHEN¹, Cheng-Xiang WANG²,
John THOMPSON³ & Jing ZHANG^{1*}

¹*School of Electronics Information and Communications, Huazhong University of Science and Technology, Wuhan 430074, China;*

²*Joint Research Institute for Signal and Image Processing, School of Engineering & Physical Sciences, Heriot-Watt University, Edinburgh EH14 4AS, UK;*

³*Institute for Digital Communications, University of Edinburgh, Edinburgh EH9 3JL, UK*

Received August 22, 2015; accepted November 23, 2015; published online December 22, 2015

Abstract It is important to assess the effect of transmit power allocation schemes on the energy consumption on random cellular networks. The energy efficiency of 5G green cellular networks with average and water-filling power allocation schemes is studied in this paper. Based on the proposed interference and achievable rate model, an energy efficiency model is proposed for MIMO random cellular networks. Furthermore, the energy efficiency with average and water-filling power allocation schemes are presented, respectively. Numerical results indicate that the maximum limits of energy efficiency are always there for MIMO random cellular networks with different intensity ratios of mobile stations (MSs) to base stations (BSs) and channel conditions. Compared with the average power allocation scheme, the water-filling scheme is shown to improve the energy efficiency of MIMO random cellular networks when channel state information (CSI) is attainable for both transmitters and receivers.

Keywords energy efficiency, cellular networks, MIMO, achievable rate model, power allocation scheme

Citation Ge X H, Chen J Q, Wang C X, et al. 5G green cellular networks considering power allocation schemes. *Sci China Inf Sci*, 2016, 59(2): 022308, doi: 10.1007/s11432-015-5502-8

1 Introduction

A more than ten-fold increase in mobile data traffic between 2013 and 2018 is predicted in recent forecasts from Cisco [1]. Corresponding to this growth rate in mobile communications, 15%–20% energy consumption for the entire information and communications technologies (ICT) industry, as well as 0.3%–0.4% of annual global carbon dioxide emissions will be increased [2]. Considering the significant proportion of mobile data traffic, it is important to more deeply analyze the energy efficiency of 5G green cellular networks and provide some guidelines for future power allocation scheme in the fifth generation (5G) cellular networks.

With the development of wireless transmission technologies, multi-input multi-output (MIMO) antenna technology is widely used to improve the capacity of wireless communication systems. Moreover, numerous energy efficiency models have been investigated for MIMO communication systems in [3–11]. To

* Corresponding author (email: zhangjing@mail.hust.edu.cn)

maximize the energy efficiency of MIMO communication systems over time varying channels, the impact of line-of-sight, out-of-cell interferers and the antenna correlation was discussed for downlink channels in [3]. An optimal power control algorithm was proposed for the generalized energy-efficiency proportional fair metric in a multiuser MIMO communication system [4]. A tight upper bound of the energy efficiency with a spectrum efficiency constraint was derived for a virtual-MIMO communication system which has one destination and one relay using the compress-and-forward (CF) cooperation scheme [5]. Based on the proposed energy efficiency upper bound, the optimal power and bandwidth allocation have been derived for maximizing the energy efficiency of MIMO communication systems. In [6], an energy efficient adaptive transmission scheme was proposed for MIMO beamforming communication systems with orthogonal space-time block coding (OSTBC) with imperfect channel state information (CSI) at transmitters. An algorithm that jointly considering the transmit power, power allocation among streams and beamforming matrices was developed to maximize the energy efficiency of MIMO communication systems with interference channels [7]. Due to the trade-off between the traffic rate and the hardware power consumption, an antenna selection algorithm was developed in MIMO communication systems [8]. By jointly choosing the transmission power and precoding vector among codebooks, a radio resource optimization scheme was proposed to improve the spectrum and energy efficiency of MIMO communication systems with user fairness constraints [9]. Assuming that channel state information is known to the transmitters, an optimal power control scheme was proposed for maximizing the energy efficiency of a base station (BS) using multiple antennas [10]. Considering distributed transmitter systems employing a zero-forcing based multiuser MIMO precoding, a heuristic power control method was proposed to improve the energy efficiency of MIMO communication systems under constraints on the per-user target rate and the per-antenna instantaneous transmit power [11]. However, the above studies concerning the energy efficiency of MIMO communication systems have been limited to finite numbers of interfering transmitters.

Many studies indicated that improving the energy efficiency of cellular networks is a critical problem for the future of the telecommunication industry [12–20]. The purpose of traditional cellular wireless communications always is higher throughput for the user and higher capacity for the service provider, regardless of energy efficiency. Davaslioglu and Ayanoglu discussed the specific reasons for inefficiency and potential improvement in the physical layer as well as in more higher layers of the communication protocol of cellular networks [12]. Hasan et al. presented a review of methods of improving the energy efficiency of cellular networks, and explored some related topics and challenges, moreover suggested some techniques to make green cellular networks possible [13]. A novel user cooperation scheme termed inter-network cooperation was investigated to improve uplink emission energy efficiency of cellular networks with the help of a short-range communication network [14]. Three typical multi-cell cooperation scenarios, i.e., the energy efficiency coordinated multi-point transmissions, the traffic-intensity-aware and the energy-aware multi-cell cooperation were also discussed for reducing the energy consumption of cellular networks in [15]. The downlink performance evaluation of small cell networks including capacity and energy efficiency was investigated in [16], where BSs and users are modeled as two independent spatial Poisson point processes. In related work on a MIMO cellular network with one single macrocell base station (MBS) and multiple femtocell access points, an opportunistic interference alignment scheme was proposed for reducing the intra and inter tier interference and the energy consumption [17]. Through the deployment of sleeping strategies and small cells, the success probability and energy efficiency were improved for homogeneous macrocell single tier wireless networks and heterogeneous multiple tiers wireless networks in [18]. Using the signal-to-interference-and-noise ratio (SINR) as the function of the user's location, an analytical model was proposed for calculating the spectrum and energy efficiency of cellular networks with orthogonal frequency division multiplexing access (OFDMA) [19]. Based on single antenna transmission systems, the energy efficiency of random cellular networks with the statistical analysis of traffic load and power consumption was also evaluated in [20].

However, in future 5G mobile communication systems, the energy efficiency is proposed as one of the most important performance indicators [21–23]. Considering that the 5G network will be a huge multi-layer multi-RAT Het-Net network [24], simple scenarios such as MIMO communication systems

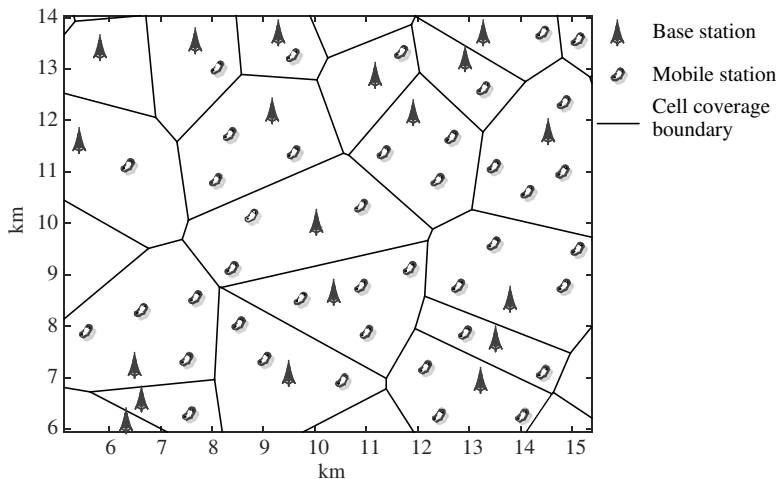


Figure 1 Illustration of PVT random cellular networks.

considering finite interfering transmitters in one single cell are so simple that have no ability to accurately evaluate the energy efficiency of complex cellular networks. Moreover, studies of the impact of different power allocation schemes, which is the important influence factor in power consumption evaluation, on the energy efficiency of MIMO random cellular networks are surprisingly rare in the open literature. Motivated by the previous issues, we investigate the energy efficiency of MIMO random cellular networks with different power allocation schemes in this paper. The contributions and novelties are summed up as follows.

(1) A random cellular network using stochastic geometry theory for MIMO transmitters and receivers is proposed for evaluating the network level energy efficiency considering different power allocation schemes.

(2) We propose an interference model and compute the achievable rate of MIMO PVT random cellular networks with infinite interfering BSs which distributing as a Poisson point process, taking effects of path loss, fading and shadowing in radio propagation channels into account.

(3) With the proposed interference and achievable rate model, performance analysis for energy efficiency of MIMO PVT random cellular networks with average and water-filling power allocation schemes has been derived.

(4) Based on the simulation results, the impact of average and water-filling power allocation schemes on the energy efficiency of MIMO PVT random cellular networks has been analyzed and compared in detail.

2 System model

Assume that in the infinite plane \mathbb{R}^2 , BSs and MSs are deployed randomly, of which the locations are approximated to be two independent Poisson point processes [25] with intensities λ_M and λ_B , which are expressed as

$$\Pi_B = \{y_{Bi}, i = 0, 1, 2, \dots\}, \Pi_M = \{x_{Mj}, j = 0, 1, 2, \dots\}, \quad (1)$$

where y_{Bi} and x_{Mj} are two-dimensional location coordinates of the i th BS BS_i and the j th MS MS_j , respectively.

Assume that MSs communicate with the closest BS for suffering the minimum path loss in the process of radio propagation. All other BSs in the infinite plane \mathbb{R}^2 are interfering BSs. The OFDMA scheme is adopted for wireless transmission to avoid the intra-interference in the cell. Thus, we can split the plane \mathbb{R}^2 into a number of irregular polygons approximately expressing coverage areas of different cells through the Delaunay Ttiangulation method [26]. The illustration of stochastic and irregular topology in Figure 1 is so-called Poisson Voronoi Tessellation (PVT) random network, where each cell is identified by C_i ($i = 0, 1, 2, \dots$).

According to Palm theory, one of the most important features of PVT random cellular networks is that geometric characteristics of all cells coincide with each other, such that can be viewed as coinciding with a typical PVT cell C_0 [27]. Thus, analytical results for a typical PVT cell C_0 can reveal properties of the whole PVT random cellular network.

Assume that each BS is integrated with N_t transmission antennas and each MS is equipped with N_r receive antennas. In this paper, our study is focused on the downlinks of cellular wireless communication systems. Without loss of generality, the signal received at an MS MS_0 in the typical PVT cell C_0 is expressed as

$$\mathbf{y}_0 = \mathbf{H}_{00}\mathbf{x}_0 + \sum_{i=1}^{\infty} \mathbf{H}_{i0}\mathbf{x}_i + \mathbf{n}_0 = \mathbf{H}_{00}\hat{\mathbf{V}}_0\mathbf{A}_0\mathbf{c}_0 + \sum_{i=1}^{\infty} \mathbf{H}_{i0}\hat{\mathbf{V}}_i\mathbf{A}_i\mathbf{c}_i + \mathbf{n}_0, \quad (2)$$

where \mathbf{c}_0 is N_t dimension desired transmitted symbol satisfying $\mathbf{c}_0^H\mathbf{c}_0 = 1$ from the BS BS_0 , \mathbf{c}_i ($i = 1, 2, \dots$) is the interfering transmitted symbol satisfying $\mathbf{c}_i^H\mathbf{c}_i = 1$ from the interfering BS BS_i ($i = 1, 2, \dots$), $\mathbf{A}_i = \text{diag}(\sqrt{P_{i1}}, \sqrt{P_{i2}}, \dots, \sqrt{P_{iN_t}})$ ($i = 0, 1, 2, \dots$) is $N_t \times N_t$ transmit power allocation vector satisfying $\sum_{j=1}^{N_t} P_{ij} = P_{Ti}$. The scalars P_{T0} and P_{Ti} ($i = 1, 2, \dots$) denote the transmission power at the desired BS BS_0 and the interfering BS BS_i respectively. Afterwards, the transmitted symbol vector is precoded by an $N_t \times N_t$ matrix $\hat{\mathbf{V}}_i$ as $\mathbf{x}_i = \hat{\mathbf{V}}_i\mathbf{A}_i\mathbf{c}_i$ ($i = 0, 1, 2, \dots$); \mathbf{H}_{00} is the $N_r \times N_t$ channel matrix between the MS MS_0 and the desired BS BS_0 , \mathbf{H}_{i0} ($i = 1, 2, 3, \dots$) is the $N_r \times N_t$ channel matrix between the MS MS_0 and the interfering BS BS_i , the element $h_{0,k,n}$ ($k = 1, 2, \dots, N_r; n = 1, 2, \dots, N_t$) of channel matrix \mathbf{H}_{00} and the element $h_{i,k,n}$ ($i = 1, 2, \dots; k = 1, 2, \dots, N_r; n = 1, 2, \dots, N_t$) of channel matrix \mathbf{H}_{i0} are independently and identically distributed (i.i.d.)¹⁾; \mathbf{n}_0 is the N_r dimension additive white Gaussian noise (AWGN) vector in the wireless channel, the noise power is equal to N_0 . Due to the infinite sum of interferers in Eq. (2), it is reasonable to assume that the system model of MIMO PVT random cellular networks is an interference limited scenario.

3 Achievable rate of MIMO PVT random cellular networks

3.1 Interference model

The received signals including the interference signals are assumed to be propagated through independent wireless channels [29]. The shadowing effect is assumed to follow a log-normal distribution, to which a Gamma fading distribution is an alternative approximately [30] for simplifying calculation. The multi-path fading is assumed to be follow a Nakagami-m distribution which spans via the m parameter the widest range of the amount of fading (from 0 to 2) among all the multi-path distributions [31]. In this case, the wireless channel gain from the n th transmission antenna at the interfering BS BS_i to the k th receive antenna at the MS MS_0 is expressed as

$$||h_{i,k,n}||^2 = \frac{1}{R_i^\sigma} w_{i,k,n} |z_{i,k,n}|^2, \quad (3)$$

where R_i is the Euclidean distance between the MS MS_0 and the interfering BS BS_i , σ is the path loss coefficient in radio propagation, $w_{i,k,n}$ is a random variable governed by Gamma distribution, and $z_{i,k,n}$ is a random variable governed by Nakagami-m distribution.

Considering that the OFDMA scheme and a relevant interference cancellation scheme [32] are used for intra-cell signals, there is no significant co-channel interference from within one PVT cell [33]. Therefore, the co-channel interference is assumed to be transmitted from all BSs in the infinite plane except for the BS in typical PVT cell C_0 . Assume that the active interfering BSs set is modeled an independent thinning process on the BS Poisson point process, which still form a Poisson point process with intensity

¹⁾ Our analysis can also approximate fading correlation scenarios by performing moment matching to simplify to a single Gamma distribution [28].

λ_{inf} [20], and generally satisfies $0 \leq \lambda_{\text{inf}} \leq \lambda_{\text{B}}$. Therefore, the interference power aggregated at the MS MS_0 is expressed as [34]

$$P_I = \sum_{k=1}^{N_r} \left(\sum_{i=1}^{\infty} \frac{I_{i,k}}{R_i^\sigma} \right) = \sum_{i=1}^{\infty} \frac{I_i}{R_i^\sigma} = \sum_{i \in \Pi_{\text{inf}}} \frac{I_i}{R_i^\sigma}, \quad (4a)$$

with

$$I_i = \sum_{k=1}^{N_r} (I_{i,k}), \quad (4b)$$

where $I_{i,k}$ is the received interference of the k th antenna of the MS MS_0 from the i th BS regardless of the pass loss fading. Considering that every antenna of the MS MS_0 will receive multiple interference streams transmitted from N_t antennas of interfering BSs, I_i represents the interference power received by N_r antennas at the MS MS_0 , which is further expressed as [35]

$$I_i = P_{Ti} \sum_{k=1}^{N_r} \sum_{n=1}^{N_t} T_{i,k,n}, \quad (5a)$$

with

$$T_{i,k,n} = w_{i,k,n} |z_{i,k,n}|^2. \quad (5b)$$

Assume that the average power of interference terms that are transmitted from the n th antenna of interfering BS BS_i and received at the k th antenna of MS MS_0 are approximately equal in the statistical meaning [36]. Thus, the Gamma fading over all sub-channels is simplified as $w_{i,k,n} (i = 1, 2, \dots; k = 1, 2, \dots, N_r; n = 1, 2, \dots, N_t) = w_i$. Furthermore, the interference power received by N_r antennas of the MS MS_0 is derived by

$$I_i = P_{Ti} H_i, \quad (6a)$$

with

$$H_i = w_i \sum_{k=1}^{N_r} \sum_{n=1}^{N_t} |z_{i,k,n}|^2. \quad (6b)$$

A channel that experiences the product of both Gamma fading and Nakagami fading follows a K_G distribution. Therefore, the PDF of H_i is derived by [30, 37, 38]

$$f_{H_i}(y) = \frac{2 \left(\frac{m\lambda}{\Omega} \right)^{\frac{N_t N_r m + \lambda}{2}}}{\Gamma(N_t N_r m) \Gamma(\lambda)} y^{\frac{N_t N_r m + \lambda - 2}{2}} K_{\lambda - N_t N_r m} \left(2 \sqrt{\frac{m\lambda y}{\Omega}} \right) (y > 0, i = 1, 2, 3, \dots), \quad (7a)$$

with

$$\Omega = \sqrt{(\lambda + 1)/\lambda} \quad \lambda = 1 / \left(e^{(\sigma_{dB}/8.686)^2} - 1 \right)^2, \quad (7b)$$

where $\Gamma(\cdot)$ is a Gamma function, m is a Nakagami shaping factor, $K_{\lambda-m}(\cdot)$ is the modified Bessel function of the second kind with order $\lambda - m$ and σ_{dB} is the variance of shadowing effect values.

Based on Eq. (4a) and the Campbell theory in [26], the characteristic function of the interference power aggregated at the MS MS_0 can be written as

$$\begin{aligned} \Phi_{P_I} &= \mathbb{E} \left\{ e^{j\omega P_I} \right\} = \exp \left(-2\pi\lambda_{\text{inf}} \iint \left(1 - e^{-\frac{j\omega y}{R^\sigma}} \right) f_I(y) dy R dR \right) \\ &= \exp \left(-2\pi\lambda_{\text{inf}} \int_{\mathbb{R}^+} \left[1 - \phi_I \left(\frac{\omega}{R^\sigma} \right) \right] R dR \right), \end{aligned} \quad (8)$$

where $f_I(y)$ and $\phi_I(\omega)$ are the PDF and the characteristic function of the total interference power I_i received at the MS MS_0 , respectively; $\mathbb{E} \{ \cdot \}$ is the expectation operation. Based on the result in [34], the characteristic function Φ_{P_I} represents a α stable random process, which can be simply denoted as

$P_I \sim \text{Stable}(\alpha = 2/\sigma, \beta = 1, \delta, \mu = 0)$, where α and δ are the stability parameter and the scale parameter, respectively. Based on the α stable characteristic function expression, Φ_{P_I} can be re-written as

$$\Phi_{P_I} = \exp \left\{ -\delta |\omega|^\alpha \left[1 - j\beta \text{sign}(\omega) \tan \left(\frac{\pi\alpha}{2} \right) \right] \right\}, \quad (9a)$$

with

$$\delta = \lambda_{\text{inf}} \frac{\pi \Gamma(2 - \alpha) \cos \left(\frac{\pi\alpha}{2} \right)}{1 - \alpha} \text{E} \{ P_{T_i}^\alpha \} \text{E} \{ H_i^\alpha \} \quad (\alpha \neq 1, i = 1, 2, 3, \dots), \quad (9b)$$

where $\text{E} \{ P_{T_i}^\alpha \}$ is the moment of the receiving power raised to the power α at the MS MS_0 . Based on Eq. (7a), $\text{E} \{ H_i^\alpha \}$ is expressed as

$$\text{E} \{ H_i^\alpha \} = \int_0^\infty \frac{2 \left(\frac{m\lambda}{\Omega} \right)^{\frac{N_t N_r m + \lambda}{2}}}{\Gamma(N_t N_r m) \Gamma(\lambda)} y^{\frac{N_t N_r m + \lambda - 2}{2}} K_{\lambda - N_t N_r m} \left(2\sqrt{\frac{m\lambda y}{\Omega}} \right) y^\alpha dy. \quad (10)$$

From the table of integrals in [38], Eq. (10) can be written in closed form as

$$\text{E} \{ H_i^\alpha \} = \left(\frac{m\lambda}{\Omega} \right)^{-\alpha} \frac{\Gamma(\lambda + \alpha) \Gamma(N_t N_r m + \alpha)}{\Gamma(N_t N_r m) \Gamma(\lambda)} \quad (i = 0, 1, 2, 3, \dots). \quad (11)$$

Substituting Eq. (11) into (9b), the PDF of the interference power aggregated at the MS MS_0 can be written as

$$f_{P_I}(y) = \frac{1}{2\pi} \int_{-\infty}^{+\infty} \Phi_{P_I}(j\omega) \exp(-2\pi j\omega y) d\omega. \quad (12)$$

3.2 Achievable rate model

Based on the proposed interference model of MIMO random cellular networks in (12), the achievable rate at the MS is derived in this section. We assume the network is interference rather than noise limited, due to the infinite sum of interferers in Eq. (2) [35]. Therefore, the received signal-to-interference ratio (SIR) at the MS MS_0 in the typical PVT cell C_0 is expressed as

$$\text{SIR}_0 = \frac{\mathbf{c}_0^H \mathbf{A}_0^H \hat{\mathbf{V}}_0^H \mathbf{H}_{00}^H \mathbf{H}_{00} \hat{\mathbf{V}}_0 \mathbf{A}_0 \mathbf{c}_0}{P_I}, \quad (13)$$

where H is the conjugate transpose operation. Furthermore, the achievable rate at the MS MS_0 is expressed as

$$\mathcal{R}_0 = B_W \log [1 + \text{SIR}_0] = B_W \log \left[1 + \frac{\mathbf{c}_0^H \mathbf{A}_0^H \hat{\mathbf{V}}_0^H \mathbf{H}_{00}^H \mathbf{H}_{00} \hat{\mathbf{V}}_0 \mathbf{A}_0 \mathbf{c}_0}{P_I} \right], \quad (14)$$

where B_W is the bandwidth allocated for the MS MS_0 .

Transmitters are assumed to obtain the CSI from receivers without delay via uplink feedback channels. Moreover, the MIMO channel is divided into a number of parallel single-input single-output (SISO) channels by the single value decomposition (SVD) method. In this case, the channel matrix \mathbf{H}_{00} in Eq. (2) can be decomposed as

$$\mathbf{H}_{00} = \mathbf{U}_{00} \mathbf{D}_{00} \mathbf{V}_{00}^H, \quad (15)$$

where $\mathbf{D}_{00} = \text{diag}(\sqrt{\lambda_1}, \sqrt{\lambda_2}, \dots, \sqrt{\lambda_L})$ is the $L \times L$ diagonal matrix, $\lambda_1 \leq \lambda_2 \leq \dots \leq \lambda_L$ are eigenvalues of the matrix $\mathbf{H}_{00}^H \mathbf{H}_{00}$, and $L = \text{rank}(\mathbf{H}_{00})$ is the rank of \mathbf{H}_{00} , \mathbf{U}_{00} is the $N_r \times L$ unitary matrix, \mathbf{V}_{00} is the $L \times N_t$ unitary matrix. Furthermore, assuming that the full matrix $\mathbf{V}_{00} = \hat{\mathbf{V}}_0$, the achievable rate at the MS MS_0 is expressed as

$$\mathcal{R}_0 = B_W \log \left[1 + \frac{\mathbf{c}_0^H \mathbf{A}_0^H \mathbf{D}_{00}^2 \mathbf{A}_0 \mathbf{c}_0}{P_I} \right] = B_W \log \left[1 + \frac{\mathbf{A}_0^H \mathbf{D}_{00}^2 \mathbf{A}_0}{P_I} \right]. \quad (16)$$

4 Green MIMO random cellular networks

Considering that the MS required traffic load will influence the BS transmission power, the energy efficiency of MIMO PVT cellular networks will be related with the traffic rates in MSs. In this section, we discuss this relationship in more detail. Two classical power control schemes are discussed with the proposed model, numerical results show inherent relationships among the energy efficiency, traffic load, and the prevailing channel environment conditions.

4.1 Basic energy efficiency model

In this paper, we define the energy efficiency of MIMO PVT cellular networks as the average ratio of traffic load over total power consumption at a BS in a typical PVT cell C_0 [39] based on Palm theory [26]

$$EE = \frac{r(P)}{P(P)_s} = \frac{\mathbb{E}\{\Gamma_{C_0}\}}{\mathbb{E}\{P_{BS}\}} \left[\frac{\text{nat}}{\text{Joule}} \right], \quad (17)$$

where Γ_{C_0} is the traffic rate in a typical PVT cell C_0 , P_{BS} is the total power consumed at a BS in a typical PVT cell C_0 . The total BS power consumption includes both fixed power and dynamic power consumption terms [40]. According to [41], the total power consumption P_{BS} is written following

$$P_{BS} = \frac{P_{C_0\text{-real}}}{\eta} + N_t P_{\text{dyn}} + P_{\text{sta}}, \quad (18)$$

where $P_{C_0\text{-real}}$ is the total BS radio frequency transmission power for all transmit antennas, η is the average efficiency of the BS power amplifiers, N_t is the number of active BS antennas, P_{dyn} is the RF circuit power for an antenna and P_{sta} is the fixed power consumption in a BS. Moreover, there is a maximal BS transmission power P_{max} in practical. In this case, when the required BS transmission power exceeds P_{max} the corresponding transmission traffic will be interrupted. Therefore, the average transmission traffic rate is calculated by $\mathbb{E}\{\Gamma_{C_0}\} F_{P_{C_0}}(P_{\text{max}})$, where $F_{P_{C_0}}(P_{\text{max}})$ is the probability that the BS transmission power less than P_{max} . Furthermore, the energy efficiency of the MIMO PVT random cellular networks is expressed as

$$EE = \frac{\mathbb{E}\{\Gamma_{C_0}\} F_{P_{C_0}}(P_{C_0\text{-max}})}{\mathbb{E}\{P_{BS}\}} = \frac{\mathbb{E}\{\Gamma_{C_0}\} F_{P_{C_0}}(P_{C_0\text{-max}})}{\frac{1}{\eta} \mathbb{E}\{P_{C_0\text{-real}}\} + N_T P_{\text{dyn}} + P_{\text{sta}}}, \quad (19)$$

where $\mathbb{E}\{P_{C_0\text{-real}}\}$ is the average BS actual transmission power in the typical PVT cell C_0 .

Many empirical measurement results have demonstrated that the traffic load in both wired and wireless networks, including cellular networks, is self-similar and bursty. Considering the infinite variance characteristic of self-similar distributions, Pareto distributions with infinite variance were proposed for modeling the self-similar traffic in wireless networks [42]. Therefore, the traffic rate $\rho(x_{M_i})$ at the MS MS_i is assumed to be a Pareto distribution with infinite variance. Traffic rates of all MSs are assumed to be i.i.d. Then, the PDF of traffic rate is expressed by

$$f_\rho(x) = \frac{\theta \rho_{\min}^\theta}{x^{\theta+1}}, \quad x \geq \rho_{\min} > 0, \quad (20)$$

where $\theta \in (1, 2]$ is a shape parameter, also known as the tail index. ρ_{\min} is minimum possible value of traffic rate that is needed to meet the MS's quality of service (QoS) requirements. Furthermore, the average traffic rate at an MS is expressed as

$$\mathbb{E}\{\rho\} = \frac{\theta \rho_{\min}}{\theta - 1}. \quad (21)$$

Based on the results in [29], the average traffic rate for all MSs in a typical PVT cell C_0 is denoted as $\mathbb{E}\{\Gamma_{C_0}\} = \frac{\lambda_M \theta \rho_{\min}}{\lambda_B (\theta - 1)}$. As a consequence, the energy efficiency of MIMO PVT random cellular networks is derived by

$$EE = \frac{\frac{\lambda_M \theta \rho_{\min}}{\lambda_B (\theta - 1)} F_{P_{C_0}}(P_{C_0\text{-max}})}{\frac{1}{\eta} \mathbb{E}\{P_{C_0\text{-real}}\} + N_T P_{\text{dyn}} + P_{\text{sta}}}. \quad (22)$$

4.2 Energy efficiency of MIMO cellular networks using average power allocation scheme

The average power allocation scheme is a simple antenna power control scheme which has been widely used for practical MIMO wireless communications systems. The maximum ratio transmission / maximum ratio combining (MRT/MRC) methods are assumed to be adopted in MIMO PVT random cellular networks [43], the achievable rate with an average power allocation scheme satisfying $\mathbf{A}_0 = \frac{P_0}{N_t} \mathbf{I} (N_t)$ at the MS MS_0 in the typical PVT cell C_0 is derived as

$$\begin{aligned} \mathcal{R}_l &= B_W \log \left[1 + \frac{\mathbf{A}_0^H \mathbf{D}_{00}^2 \mathbf{A}_0}{P_I} \right] \\ &\leq B_W \log \left[1 + \frac{\frac{P_0}{N_t} \lambda_{\max}(\mathbf{H}_{00}^H \mathbf{H}_{00})}{P_I} \right] = B_W \log \left[1 + \frac{\frac{P_0}{N_t} \lambda_{\text{rank}}(\mathbf{H}_{00})}{P_I} \right] \\ &\leq B_W \log \left[1 + \frac{\frac{P_0}{N_t} \|\mathbf{H}_{00}\|_F^2}{P_I} \right] = B_W \log \left[1 + \frac{\frac{P_0}{N_t} \sum_{k=1}^{N_r} \sum_{n=1}^{N_t} |h_{0,k,n}|^2}{P_I} \right] \\ &\approx B_W \log \left[1 + \frac{\frac{P_0}{N_t} \sum_{k=1}^{N_r} \sum_{n=1}^{N_t} \frac{1}{R_0^\sigma} w_0 |z_{0,k,n}|^2}{P_I} \right] = B_W \log \left[1 + \frac{\frac{P_0}{N_t} \frac{H_0}{R_0^\sigma}}{P_I} \right], \end{aligned} \quad (23)$$

where $\lambda_{\max}(\mathbf{H}_{00}^H \mathbf{H}_{00})$ is the maximum eigenvalue operation for the matrix $\mathbf{H}_{00}^H \mathbf{H}_{00}$, R_0 is the Euclidean distance between the BS BS_0 and the MS MS_0 , w_0 is the shadowing fading over sub-channels between the BS BS_0 and the MS MS_0 , $|z_{0,k,n}|$ is the Nakagami fading over the sub-channel between the n th antenna of the BS BS_0 and the k th antenna of the MS MS_0 . Let $\tau = \frac{P_0}{N_t} \frac{H_0}{R_0^\sigma} / P_I$, the relationship between achievable rate and traffic rate of MS_0 is regarded as

$$B_W \log_2(1 + \tau) = \rho(x_{M0}). \quad (24)$$

Based on the PDF of traffic rate in Eq. (20), the PDF of τ is derived as

$$f_\tau(z) = \frac{\theta \rho_{\min}^\theta B_W^{-\theta}}{\ln 2 \cdot (1+z)} (\log_2(1+z))^{-\theta-1} \left(z > z_0 = 2^{\rho_{\min}/B_W} - 1 \right). \quad (25)$$

Consider that the MS communicates with the closest BS in a PVT cell. Furthermore the probability of the Euclidean distance between an MS and the i th near BS can be expressed as

$$\Pr(i-1 \text{ BSs in a circle area with radius } R) = \frac{(\lambda_B \pi R^2)^{i-1}}{(i-1)!} e^{-\lambda_B \pi R^2}, \quad (26)$$

where $\Pr(\cdot)$ is the probability operation. Thus, the PDF of the distance R is derived by

$$f_{R_0}(R) = \frac{d \Pr\{R_0 \leq R\}}{dR} = -\frac{d \Pr\{R_0 > R\}}{dR} = -\frac{d \left(\frac{(\lambda_B \pi R^2)^0 e^{-\lambda_B \pi R^2}}{0!} \right)}{dR} = 2\pi \lambda_B R e^{-\pi \lambda_B R^2}, \quad (27)$$

where $\Pr\{R_0 > R\}$ is the probability that there is not a BS in the circular area with the center x_{M0} and the radius R . Considering the path loss effect on the distance R , the corresponding PDF is derived as

$$f_{R_0^\sigma}(R) = \frac{1}{\sigma} R^{\frac{2}{\sigma}-1} \cdot 2\pi \lambda_B e^{-\pi \lambda_B R^{2/\sigma}}. \quad (28)$$

Furthermore, the downlink transmission power P_0 between the BS BS_0 and the MS MS_0 is expressed as

$$P_0 = P_I \cdot \frac{N_t \cdot R_0^\sigma \cdot \tau}{H_0}. \quad (29)$$

Based on Eqs. (12) (25) (28) and (29), the characteristic function of P_0 is derived by

$$\phi_{P_0}(\omega) = \int_x \phi_{P_I}(\omega x) f_{\frac{N_t R_0^\sigma \tau}{H_0}}(x) dx$$

$$\begin{aligned}
 &= \int_x \int_{y,z} \frac{y \phi_{P_I}(\omega x)}{z N_t} f_\tau(z) f_{R_0^\sigma} \left(\frac{xy}{z N_t} \right) f_{H_0}(y) dx dy dz \\
 &= \int_{y,z} \frac{\pi \lambda_B}{G(\omega) z^{\frac{2}{\sigma}} y^{\frac{-2}{\sigma}} + \pi \lambda_B} f_{H_0}(y) f_\tau(z) dy dz,
 \end{aligned} \tag{30a}$$

with

$$G(\omega) = \delta |\omega|^{2/\sigma} [1 - j \cdot \text{sign}(\omega) \cdot \tan \frac{\pi}{\sigma}], \tag{30b}$$

where $f_{H_0}(y)$ is the PDF of the channel variable $H_0 = w_0 \sum_{n=1}^{N_t} \sum_{k=1}^{N_r} |z_{0,k,n}|^2$. In this paper, the channel variable H_i is i.i.d. for all channels. Based on Eq. (7a), the function $f_{H_0}(y)$ is expressed by

$$f_{H_0}(y) = \frac{2 \left(\frac{m\lambda}{\Omega} \right)^{\frac{N_t N_r m + \lambda}{2}}}{\Gamma(N_t N_r m) \Gamma(\lambda)} y^{\frac{N_t N_r m + \lambda - 2}{2}} K_{\lambda - N_t N_r m} \left(2 \sqrt{\frac{m\lambda y}{\Omega}} \right) (y > 0). \tag{31}$$

Assume that BS transmission power is dynamically adjusted to meet the required traffic rates for all MSs in the typical PVT cell C_0 . The required BS transmission power for all MSs in C_0 is expressed by

$$\mathbb{P}_{C_0} \stackrel{\text{def}}{=} \sum_{x_{MS} \in \Pi_M} P_s \cdot \mathbf{1}\{x_{MS} \in C_0\}, \tag{32}$$

where P_s is the consumed power transmitted from the BS BS_0 to the MS MS_s in the typical cell C_0 , $\mathbf{1}\{\dots\}$ is an indicator function for gathering together all MSs belong to the same typical PVT cell C_0 . Assume that P_s is a series of i.i.d. random variables, of which the PDF and the characteristic function are denoted as $f_P(p)$ and $\phi_P(\omega)$, respectively. Based on the Campbell theory in [27], the characteristic function of required BS transmission power P_{C_0} in the typical PVT cell C_0 is derived as

$$\begin{aligned}
 \phi_{P_{C_0}}(\omega) &= \exp \left[\iint_{x,p} (e^{j\omega p} - 1) f_P(p) \mathbf{1}\{x \in C_0\} 2\pi \lambda_M x dp dx \right] \\
 &= \exp \left[-2\pi \lambda_M \int_0^\infty (1 - \phi_P(\omega)) (\mathbf{1}\{x \in C_0\}) x dx \right] \\
 &= \exp \left[-2\pi \lambda_M \int_0^\infty (1 - \phi_P(\omega)) e^{-\pi \lambda_B x^2} x dx \right] \\
 &= \exp \left[-\frac{\lambda_M}{\lambda_B} (1 - \phi_P(\omega)) \right].
 \end{aligned} \tag{33}$$

And $f_{P_{C_0}}(x)$ is the PDF of the required BS transmission power P_{C_0} , which can be calculated by applying the inverse Fourier operation to $\phi_{P_{C_0}}(\omega)$. Considering the limit of BS transmission power P_{\max} [20], the energy efficiency of MIMO random cellular networks with the average power allocation scheme is derived by

$$EE = \frac{\frac{\lambda_M \theta \rho_{\min}}{\lambda_B (\theta - 1)} \cdot \left(\int_0^{P_{\max}} f_{P_{C_0}}(x) dx \right)^2}{\frac{1}{\eta} \int_0^{P_{C_0-\max}} x f_{P_{C_0}}(x) dx + (N_T P_{\text{dyn}} + P_{\text{sta}}) \cdot \int_0^{P_{\max}} f_{P_{C_0}}(x) dx} \tag{34}$$

4.3 Energy efficiency of MIMO cellular networks using water-filling power allocation scheme

When perfect CSI is assumed to be available at both transmitters and receivers in wireless communication systems, the water-filling power allocation scheme is used for improve the capacity of wireless communication systems [44]. The downlink capacity over wireless channels between the BS BS_0 and the MS MS_0 is expressed as

$$\mathbb{C} = \max \log \det \left(I_{N_t} + \frac{A_0^H D_{00}^2 A_0}{P_t} \right) \quad \text{s.t.} \quad \sum_{l=1}^{N_t} P_l = P_{T0}, \tag{35}$$

where N_0 is the noise power at the transmitters. The objective function in (35) is jointly concave in the powers and this optimization problem can be solved by Lagrangian methods [45], the optimal transmission power for the l th sub-channel is given by

$$P_l = \left(\nu - \frac{N_0}{\lambda_l} \right)_+ = \frac{P_{T0}}{L} + \frac{1}{L} \sum_{l=1}^L \frac{N_0}{\lambda_l} - \frac{N_0}{\lambda_l}, \quad (36)$$

where ν is the water-filling threshold in water-filling power allocation scheme. Based on Eqs. (36) and (16), the achievable rate with the water-filling power scheme at the MS MS_0 is derived as

$$\begin{aligned} \mathcal{R}_0 &= B_W \log \left[1 + \frac{\mathbf{A}_0^H \mathbf{D}_{00}^2 \mathbf{A}_0}{P_I} \right] = B_W \log \det \left(I_{N_t} + \frac{\mathbf{A}_0^H \mathbf{D}_{00}^2 \mathbf{A}_0}{P_I} \right) \\ &= B_W \sum_{l=1}^L \log \left(1 + \frac{P_l \lambda_l}{P_I} \right) = B_W \sum_{l=1}^L \log \left(1 + \frac{\left(\frac{P_{T0}}{L} + \frac{1}{L} \sum_{l=1}^L \frac{N_0}{\lambda_l} - \frac{N_0}{\lambda_l} \right) \lambda_l}{P_I} \right). \end{aligned} \quad (37)$$

Assume that the traffic rate is satisfied by the achievable rate at the MS MS_0 , thus the corresponding balance equation is expressed by

$$B_W \sum_{l=1}^L \log \left(1 + \frac{\left(\frac{P_{T0}}{L} + \frac{1}{L} \sum_{l=1}^L \frac{N_0}{\lambda_l} - \frac{N_0}{\lambda_l} \right) \lambda_l}{P_I} \right) = \rho(x_{M0}). \quad (38)$$

When the maximal BS transmission power limit P_{\max} is considered, based on the Eq. (38) the Monte-Carlo simulation is configured to iteratively solve the transmit power P_{T0} . Then, $E\{P_{C_0\text{-real}}\}$ and $F_{P_{C_0}}(P_{\max})$ can be averaged and statistically computed from the simulation results. Substituting the values for $E\{P_{C_0\text{-real}}\}$ and $F_{P_{C_0}}(P_{\max})$ into Eq. (19), the energy efficiency of MIMO PVT cellular networks with the water-filling power allocation scheme can be obtained as

$$EE = \frac{\frac{\lambda_M \theta \rho_{\min}}{\lambda_B (\theta - 1)} (F_{P_{C_0}}(P_{\max}))^2}{\frac{1}{\eta} E\{P_{C_0\text{-real}}\} + (N_T P_{\text{dyn}} + P_{\text{sta}}) \cdot F_{P_{C_0}}(P_{\max})}. \quad (39)$$

Based on Eq. (38), the CDF and PDF of the required BS transmission power with the water-filling power allocation scheme are analyzed as follows. Unless otherwise specified, the key parameters are set as $\sigma_{dB}=6$, $\sigma=4$, $m=1$ [31], $N_t=8$, $N_r=4$, $P_{\max}=40$ Watt (W) [40], the moment of receiving power $E\{P_{T_i}^2/\sigma^2\}=10^{-2}$ W, $\lambda_B=1/(\pi \cdot 800^2)$ m $^{-2}$, $\lambda_M/\lambda_B=30$, $\lambda_{\text{inf}}=0.9\lambda_B$, $\theta=1.8$, $\rho_{\min}=2.5$ bits \cdot s $^{-1}$ \cdot Hz $^{-1}$ [20]. Figure 2 reveals the CDF of the required BS transmission power with water-filling power allocation scheme considering different path loss coefficients σ . Figure 2 indicates that the CDF curve shifts to the left with the increasing value of σ , i.e., the required BS transmission power with the water-filling power allocation scheme is decreased when the value of σ is increased in MIMO PVT random cellular networks.

Figure 3 evaluates the impact of intensity ratio of MSs to BSs λ_M/λ_B on the required BS transmission power with the water-filling power allocation scheme. Figure 3 shows that the probability mass shifts to the right when increasing the value of λ_M/λ_B , i.e., the required BS transmission power with water-filling power allocation scheme is increased when the value of λ_M/λ_B is higher.

5 Performance analysis and discussion

The effect of two power allocation schemes on the proposed energy efficiency model of MIMO random cellular networks is investigated in detail. In the following simulations, the Monte-Carlo simulation method is adopted for performance analysis. Moreover, the total BS transmission power including the required BS transmission power and RF circuit power, the BS fixed power is investigated in this section. Default system parameters are configured as: the average efficiency of power amplifier is $\eta=0.38$, the

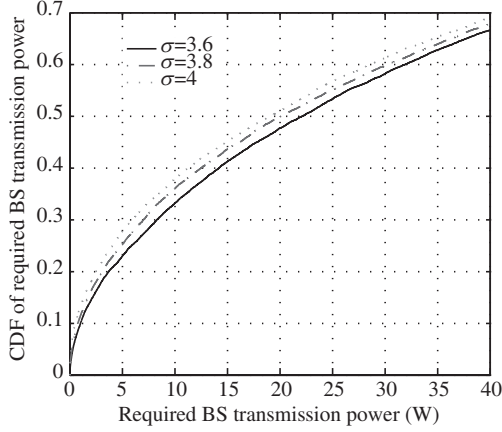


Figure 2 The CDF of the required BS transmission power with water-filling power allocation scheme.

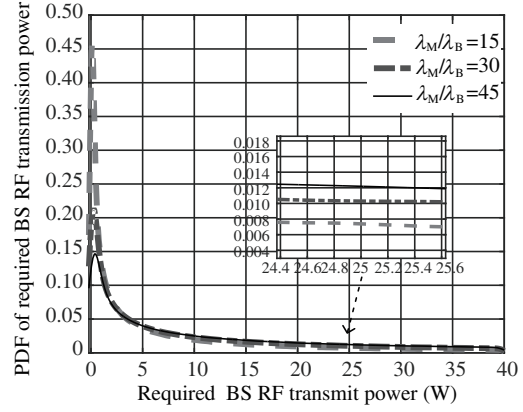


Figure 3 The PDF of the required BS transmission power with water-filling power allocation scheme.

RF circuit power for an antenna $P_{\text{dyn}} = 83 \text{ W}$ and the fixed power consumption in a BS is $P_{\text{sta}} = 45.5 \text{ W}$ [46, 47].

Figure 4 illustrates the energy efficiency of MIMO random cellular networks versus the number of transmitting antennas N_t and the intensity ratio of MSs to BSs λ_M/λ_B , where “WF” denotes the water-filling power allocation scheme and “AV” represents the average power allocation scheme. First, Figure 4 shows that the energy efficiency curve of MIMO random cellular networks shrinks down when increasing the value of N_t . Based on the result of (22), the total BS power consumption increases with the increase of the number of transmit antennas, while the average traffic rate remains unchanged. Hence, the energy efficiency of PVT random cellular networks decreases with the increase of N_t . Second, we force on one of curves and analyze the energy efficiency for both power allocation schemes with impact of λ_M/λ_B . Simulation results indicate that the water-filling/average power allocation schemes can achieve the maximum energy efficiency for MIMO random cellular networks. When the intensity ratio of MSs to BSs is low, indicating a few MSs in a typical PVT cell, the increase of the intensity ratio of MSs to BSs conduces to a moderate increase in total BS power consumption including mainly fixed BS power consumption and a small portion of dynamic BS power consumption. In this case, the energy efficiency of PVT cellular networks is increased. However, when the intensity ratio of MSs to BSs in a PVT typical cell exceeds a given threshold, a high aggregate traffic load resulted from a large number of MSs will significantly increase the total BS power consumption including mainly dynamic BS power consumption and a small portion of fixed BS power consumption. In this case, the energy efficiency of PVT cellular networks is decreased. Moreover, the energy efficiency of the water-filling power allocation scheme is always larger than for the energy efficiency of the average power allocation scheme in MIMO random cellular networks.

Figure 5 reveals the impact of the path loss coefficient σ and λ_M/λ_B on the energy efficiency of MIMO random cellular networks. The energy efficiency curve lifts up as the value of λ_M/λ_B increases. Again the energy efficiency of the water-filling power allocation scheme is always larger than for average power allocation scheme under different values of σ .

Figure 6 evaluates the effect of the minimum traffic rate ρ_{min} and the tail index θ on the energy efficiency of MIMO random cellular networks with the two power allocation schemes. There always exists a maximum energy efficiency of MIMO random cellular networks considering different system parameters. However, numerical results indicate that the energy efficiency of the water-filling power allocation scheme is always larger than for the energy efficiency of average power allocation scheme in MIMO random cellular networks.

Finally, the effect of the interfering BS intensity λ_{inf} on the energy efficiency with different power allocation schemes is investigated in Figure 7. When the values of λ_M/λ_B is fixed, the energy efficiency decreases when the value of λ_{inf} increases. The curves in Figure 7 indicate that the energy efficiency of

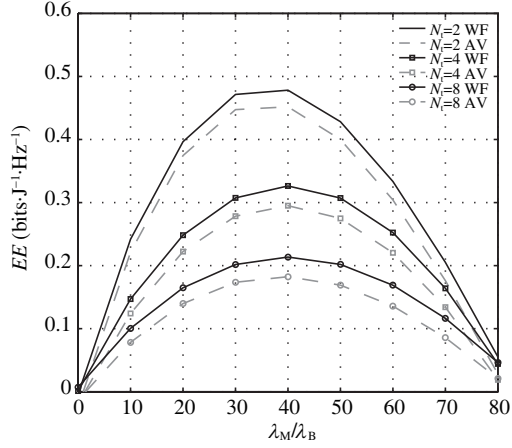


Figure 4 Energy efficiency of MIMO random cellular networks versus λ_M/λ_B and N_t .

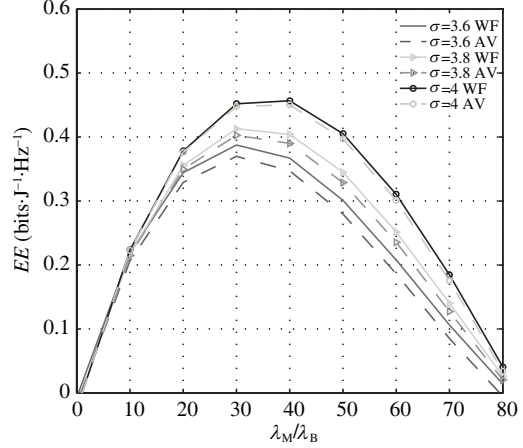


Figure 5 Energy efficiency of MIMO random cellular networks versus λ_M/λ_B and σ .

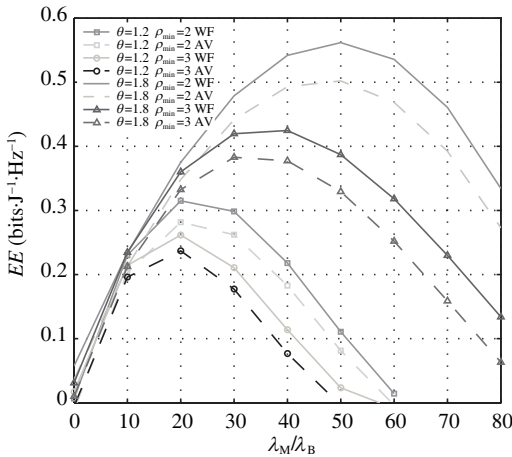


Figure 6 Energy efficiency of MIMO random cellular networks versus λ_M/λ_B , θ and ρ_{\min} .

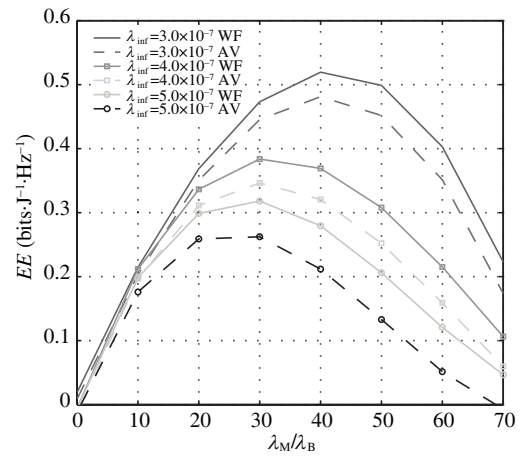


Figure 7 Energy efficiency of MIMO random cellular networks versus λ_M/λ_B and λ_{\inf} .

the water-filling power allocation scheme is always larger than for the energy efficiency of average power allocation scheme under different values of λ_{\inf} in MIMO random cellular networks. The reason is that the water-filling power allocation scheme substantially reduces the sum power, by up to 80%, in comparison to the average power allocation scheme [48]. The water-filling power allocation efficiently exploits the multiuser MIMO channels (e.g., multiuser diversity), hence power reduction is more significant. So the water-filling power allocation scheme is better than the average power allocation scheme in the energy efficiency of cellular networks when the traffic rate of MSs is the same.

6 Conclusion

In this paper, the energy efficiency of MIMO random cellular networks with different power allocation schemes is evaluated. Considering the path loss, Nakagami-m fading and shadowing effects on wireless channels, an interference model and the achievable rate of MIMO random cellular networks are first presented. Furthermore, the energy efficiency of average and water-filling power allocation schemes is proposed, respectively. Simulation results indicate that there exists a maximal network energy efficiency when considering the trade-off between intensity ratios of MSs to BSs and wireless channel conditions. When the CSI is available for both transmitters and receivers, the energy efficiency of the water-filling power allocation scheme is better than the energy efficiency of average power allocation scheme in MIMO

random cellular networks. Therefore, our results evaluate the impact of different power allocation schemes on the energy efficiency of MIMO random cellular networks. For the future work, we will use obtained results to analyze future 5G heterogeneous network adopting the millimeter wave transmission technology.

Acknowledgements This work was supported by National Natural Science Foundation of China (Grant No. 61271224), Major International (Regional) Joint Research Program of China (Grant No. 61210002), Ministry of Science and Technology (MOST) of China (Grant No. 2015FDG12580), Hubei Provincial Science and Technology Department (Grant No. 2013BHE005), EU FP7 QUICK Project (Grant No. PIRSES-GA-2013-612652), EU H2020 5G Wireless Project (Grant No. 641985), EU FP7-PEOPLE-IRSES, Project Acronym WINDOW (Grant No. 318992), and Project Acronym CROWN (Grant No. 610524), UK EPSRC (Grant No. EP/J015180/1). Ms. Peipei Song was involved in some initial discussions for this paper and we thank her useful suggestions on this paper.

Conflict of interest The authors declare that they have no conflict of interest.

References

- 1 Cisco. Cisco visual networking index: global mobile data traffic forecast update, 2013-2018. <http://www.cisco.com/c/en/us/solutions/collateral/service-provider/visual-networking-index-vni/white-paper-c11-520862.html>. 2014
- 2 Chen T, Kim H, Yang Y. Energy efficiency metrics for green wireless communications. In: Proceedings of 2010 International Conference on Wireless Communications and Signal Processing (WCSP), Suzhou, 2010. 1–6
- 3 Alfano G, Chong Z, Jorswieck E. Energy-efficient power control for MIMO channels with partial and full CSI. In: Proceedings of International ITG Workshop on Smart Antennas, Dresden, 2012. 332–337
- 4 Liu L, Miao G, Zhang J. Energy-efficient scheduling for downlink multi-user MIMO. In: Proceedings of IEEE International Conference on Communications (ICC), Ottawa, 2012. 4394
- 5 Jiang J, Dianati M, Imran M A, et al. Energy-efficiency analysis and optimization for virtual-MIMO systems. *IEEE Trans Veh Tech*, 2014, 63: 2272–2283
- 6 Chen L, Yang Y, Chen X, et al. Energy-efficient link adaptation on Rayleigh fading channel for OSTBC MIMO system with imperfect CSIT. *IEEE Trans Veh Tech*, 2013, 62: 1577–1585
- 7 Jiang C, Cimini L J. Energy-efficient transmission for MIMO interference channels. *IEEE Trans Wirel Commun*, 2013, 12: 2988–2999
- 8 Jiang C, Cimini L J. Antenna selection for energy-efficient MIMO transmission. *IEEE Wirel Commun Lett*, 2012, 1: 577–580
- 9 Garcia V, Chen C S, Lebedev N, et al. Self-optimized precoding and power control in cellular networks. In: Proceedings of IEEE 22nd International Symposium on Personal Indoor and Mobile Radio Communications, Toronto, 2011. 81–85
- 10 Chong Z, Jorswieck E. Energy-efficient power control for MIMO time-varying channels. In: Proceedings of IEEE Online Conference on Green Communications (GreenCom), New York, 2011. 92–97
- 11 Joung J, Sun S. Energy efficient power control for distributed transmitters with ZF-based multiuser MIMO precoding. *IEEE Commun Lett*, 2013, 17: 1766–1769
- 12 Davaslioglu K, Ayanoglu E. Quantifying potential energy efficiency gain in green cellular wireless networks. *IEEE Commun Surv Tut*, 2014, 16: 2065–2091
- 13 Hasan Z, Boostanimehr H, Bhargava V K. Green cellular networks: a survey, some research issues and challenges. *IEEE Commun Surv Tut*, 2011, 13: 524–540
- 14 Zou Y, Zhu J, Zhang R. Exploiting network cooperation in green wireless communication. *IEEE Trans Commun*, 2013, 61: 999–1010
- 15 Han T, Ansari N. On greening cellular networks via multicell cooperation. *IEEE Wirel Commun*, 2013, 20: 82–89
- 16 Li C, Zhang J, Letaief K. Throughput and energy efficiency analysis of small cell networks with multi-antenna base stations. *IEEE Trans Wirel Commun*, 2014, 13: 2505–2517
- 17 Nguyen T M, Shin H, Quek T Q S. Network throughput and energy efficiency in MIMO femtocells. In: Proceedings of 18th European Wireless Conference, Poznan, 2012. 1–5
- 18 Soh Y S, Quek T Q S, Kountouris M, et al. Energy efficient heterogeneous cellular networks. *IEEE J Sel Area Commun*, 2013, 31: 840–850
- 19 Karray M K. Spectral and energy efficiencies of OFDMA wireless cellular networks. In: Proceedings of IFIP Wireless Days, Venice, 2010. 1–5
- 20 Xiang L, Ge X, Wang C X, et al. Energy efficiency evaluation of cellular networks based on spatial distributions of traffic load and power consumption. *IEEE Trans Wirel Commun*, 2013, 12: 961–973
- 21 Chen M, Zhang Y, Li Y, et al. EMC: emotion-aware mobile cloud computing in 5G. *IEEE Netw*, 2015, 29: 32–38
- 22 Chen M, Hao Y, Li Y, et al. On the computation offloading at Ad Hoc cloudlet: architecture and service models. *IEEE Commun*, 2015, 53: 18–24
- 23 Chen M, Zhang Y, Hu L, et al. Cloud-based wireless network: virtualized, reconfigurable, smart wireless network to enable 5G technologies. *ACM/Springer Mobile Netw Appl*, 2015, 20: 704–712

- 24 Wang C-X, Haider F, Gao X, et al. Cellular architecture and key technologies for 5G wireless communication networks. *IEEE Commun Mag*, 2014, 52: 122–130
- 25 Yang X, Petropulu A P. Co-channel interference modeling and analysis in a Poisson field of interferers in wireless communications. *IEEE Trans Signal Process*, 2003, 51: 64–76
- 26 Ferenc J S, Nédá Z. On the size distribution of Poisson Voronoi cells. *Phys A: Stat Mech Appl*, 2007, 385: 518–526
- 27 Stoyan D, Kendall W S. *Stochastic Geometry and Its Applications*. 2nd ed. Hoboken: Wiley, 1996
- 28 Al-Ahmadi S, Yanikomeroglu H. On the approximation of the generalized-K PDF by a Gamma PDF using the moment matching method. In: *Proceedings of IEEE Wireless Communications and Networking Conference, Budapest, 2009*. 1–6
- 29 Kostic I M. Analytical approach to performance analysis for channel subject to shadowing and fading. *IEEE Proc Commun*, 2005, 152: 821–827
- 30 Bithas P S, Sagias N C, Mathiopoulos P T, et al. On the performance analysis of digital communications over generalized-K fading channels. *IEEE Commun Lett*, 2006, 10: 353–355
- 31 Simon M K, Alouini M S. *Digital Communication over Fading Channels: a Unified Approach to Performance Analysis*. Hoboken: Wiley, 2000
- 32 Dai L, Wang Z, Yang Z. Time-frequency training OFDM with high spectral efficiency and reliable performance in high speed environments. *IEEE J Sel Area Commun*, 2012, 30: 695–707
- 33 Annapureddy V S, Veeravalli V V. Sum capacity of MIMO interference channels in the low interference regime. *IEEE Trans Inf Theory*, 2011, 57: 2565–2581
- 34 Win M Z, Pinto P C, Shepp L. A mathematical theory of network interference and its applications. *Proc IEEE*, 2009, 97: 205–230
- 35 Ge X, Huang K, Wang C X, et al. Capacity analysis of a multi-cell multi-antenna cooperative cellular network with co-channel interference. *IEEE Trans Wirel Commun*, 2011, 10: 3298–3309
- 36 Alouini M S, Goldsmith A J. Area spectral efficiency of cellular mobile radio systems. *IEEE Trans Veh Tech*, 1999, 48: 1047–1066
- 37 Abdi A, Kaveh M. K distribution: an appropriate substitute for Rayleigh-lognormal distribution in fading-shadowing wireless channels. *Electron Lett*, 1998, 34: 851–852
- 38 Gradshteyn I S, Ryzhik I M. *Table of Integrals, Series, and Products*. New York: Academic Press, 2007
- 39 Chong Z, Jorswieck E. Analytical foundation for energy efficiency optimisation in cellular networks with elastic traffic. *Mobile Lightweight Wirel Syst*, 2012, 81: 18–29
- 40 Arnold O, Richter F, Fettweis G, et al. Power consumption modeling of different base station types in heterogeneous cellular networks. In: *Proceedings of IEEE Future Network and Mobile Summit, Florence, 2010*. 1–8
- 41 Yu H, Zhong L, Sabharwal A. Power management of MIMO network interfaces on mobile systems. *IEEE Trans Very Large Scale Integration (VLSI) Syst*, 2012, 20: 1175–1186
- 42 Silva A P, Mateus G R. Performance analysis for data service in third generation mobile telecommunication networks. In: *Proceedings of 35th Annual IEEE Simulation Symposium, San Deigo, 2002*. 227–234
- 43 Dighe P, Mallik R K, Jamuar S S. Analysis of transmit-receive diversity in Rayleigh fading. *IEEE Trans Commun*, 2003, 51: 694–703
- 44 Khoshnevisan M, Laneman J N. Power allocation in multi-antenna wireless systems subject to simultaneous power constraints. *IEEE Trans Commun*, 2012, 60: 3855–3864
- 45 Lu Y, Zhang W. Water-filling capacity analysis in large MIMO systems. In: *Proceeding of IEEE Computing, Communications and IT Applications Conference (ComComAp), Hong Kong, 2013*. 186–190
- 46 Xu J, Qiu L. Energy efficiency optimization for MIMO broadcast channels. *IEEE Trans Wirel Commun*, 2013, 12: 690–701
- 47 Hong X, Jie Y, Wang C-X, et al. Energy-spectral efficiency trade-off in virtual MIMO cellular systems. *IEEE J Sel Area Commun*, 2013, 31: 2128–2140
- 48 Chen R, Andrews J G, Jr Heath R W, et al. Uplink power control in multi-cell spatial multiplexing wireless systems. *IEEE Trans Wirel Commun*, 2007, 6: 2700–2711